THE JOURNAL OF PHYSICAL CHEMISTRY B
A JOURNAL OF THE AMERICAN CHEMICAL SOCIETY

pubs.acs.org/JPCB

Article

Water Structure at the Hydrophobic Nanodroplet Surface Revealed by Vibrational Sum Frequency Scattering Using Isotopic Dilution

S. Pullanchery, S. Kulik, and S. Roke*

Cite This: J. Phys. Chem. B 2022, 126, 3186−3192

Read Online

ACCESS | Metrics & More | Article Recommendations | Supporting Information

ABSTRACT: The water structure at the hydrophobic/water interface is key toward understanding hydrophobicity at the molecular level. Herein, we characterize the hydrogen-bonding network of interfacial water next to sub-micron-sized hydrophobic oil droplets dispersed in water using isotopic dilution vibrational sum frequency scattering (SFS) spectroscopy. The relative intensity of different modes, the frequency shift of the uncoupled O−D spectrum, and a low-frequency shoulder (2395 cm^{-1}) reveal that water forms an overall stronger hydrogen-bonding network next to hydrophobic droplets compared to bulk water and the air/water interface. Half of the spectral width of the oil droplet SFS spectrum is determined by inter- and intramolecular coupling of water molecules. Isotopic dilution also confirms the presence of a broad distribution (ca. 2640−2745 cm^{-1}) of non-water-hydrogen-bonded O−D modes that are red-shifted and broadened compared to similar species at the air/water interface. This band corroborates the presence of charge transfer between water and oil.

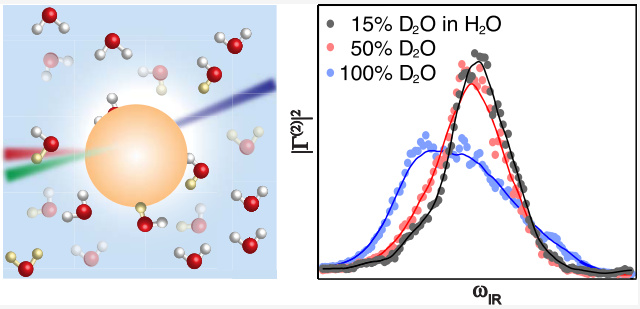

INTRODUCTION

The hydrophobic effect is responsible for various natural processes such as the formation of cell membranes, micelles, and microemulsions; stabilization of protein structures; and self-assembly of large molecular complexes.[1,2] Yet, the molecular-level understanding of water structure at a hydrophobic/water interface remains incomplete. Several theoretical studies have investigated the molecular structure of hydrophobic/water interfaces.[1,3−6] However, experimentally retrieving this information is intrinsically challenging since hydrophobic interactions result in the minimization of contact area between water and the hydrophobic phase. One of the difficulties in measuring the interfacial structure of liquid water is that one has to separate the properties of the small minority of water molecules in contact with the hydrophobic interface from the very large amount of bulk water. This information can nonetheless be obtained using vibrational sum frequency generation (SFG) spectroscopy. This method uses ultrashort laser pulses to induce a simultaneous infrared (IR) and Raman transition, which is forbidden in an isotropic bulk liquid. Vibrational SFG has been used in reflection geometry to probe planar extended liquid hydrophobic/water interfaces,[7−10] but the recorded SFG data vary dramatically throughout the literature. Based on these studies, water in contact with the same oil has either been concluded to be less strongly hydrogen (H)-bonded than bulk water[7] or more strongly H-bonded than bulk water.[10] The most likely reason for the controversially different data sets is caused by the system itself: Water does not easily wet an extended hydrophobic interface. Rather than producing a pure, homogeneously wetted hydrophobic−water interface, there are likely structural heterogeneities composed of defects (for solids) or islands/micro-lenses (for liquids) that are influenced by the intrinsically small amount of chemical impurities that even the purest liquids have.[11,12] The air/water interface is also often used as a representation of a hydrophobic interface; however, air is not a hydrophobic substance and the mere absence of a condensed phase does not replace the interactions induced by a condensed hydrophobic phase.

A solution to these issues is to use nanoscale or sub-micron-sized droplets of pure oil dispersed in water[13] and probe the droplet interfaces with vibrational sum frequency scattering (SFS,[14−18] Figure 1A). This procedure delivers surface-to-volume ratios that are 3−4 orders of magnitude higher compared to planar extended interfaces, which minimizes possible artifacts induced by impurities that are intrinsically present in any chemical compound (see refs 19−21 for an extended discussion). However, measuring the entire vibrational spectrum of interfacial water and extracting the H-bonding structure at the oil droplet/water interface is challenging for two reasons: The first limitation is caused by the absorption of the IR beam by the aqueous medium in

Received: March 22, 2022
Revised: March 31, 2022
Published: April 13, 2022

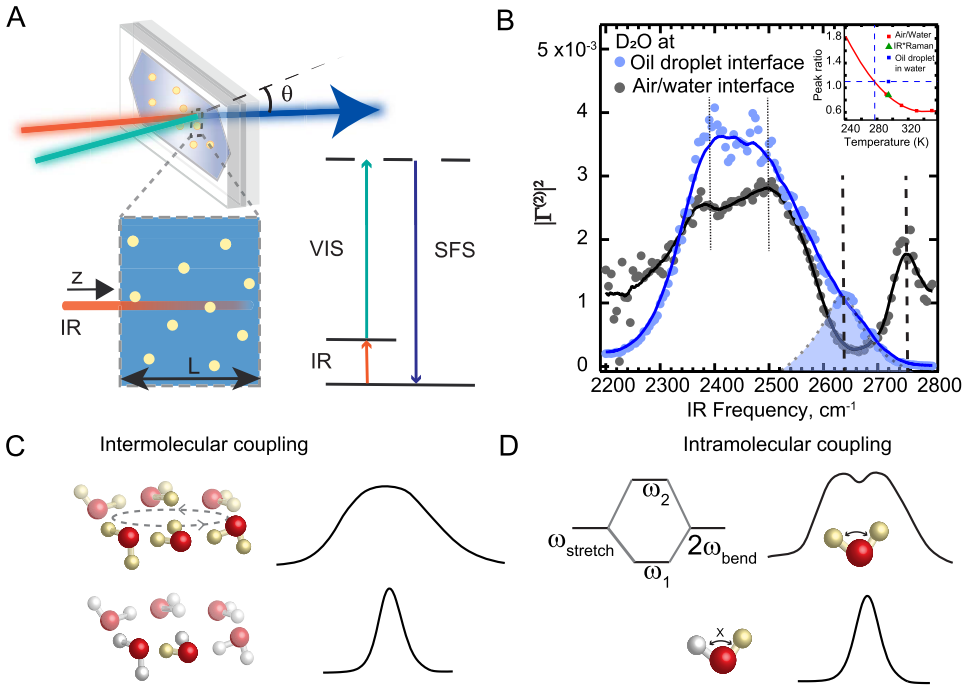

Figure 1. Vibrational SFS of oil nanodroplets in water. (A) Schematic of the vibrational SFS experiment of oil droplets dispersed in water. The zoomed-in view of the sample cross section shows the attenuation of the IR beam as it travels through the sample cell. The energy-level diagram of vibrational SFS is shown on the right. (B) Retrieved $|\Gamma^{(2)}|^2$ spectrum of 2 vol % hexadecane droplets in D_2O (blue)[23] and the reflection SFG spectrum of the air/D_2O interface (black),[10,35] measured using the SSP polarization combination. The solid lines represent the running average and are a guide to the eye. The inset shows the temperature dependence of the 2395/2500 cm^{-1} peak ratio for the air/water interface[10,35] (red squares). The green triangle corresponds to the ratio for bulk IR × Raman spectrum, and the blue rectangle corresponds to the ratio at the oil droplet surface, recorded at room temperature. Illustration of vibrational coupling effects. (C) Intermolecular coupling: When O−D modes are coupled to neighboring D_2O molecules, the vibrational energy is delocalized onto several adjacent oscillators resulting in spectral broadening (top). Isotopic dilution turns off intermolecular coupling resulting in spectral narrowing (bottom). (D) Intramolecular coupling: The symmetric stretch of D_2O ($\omega_{stretch}$) and the overtone of the D_2O bending mode ($2\omega_{bend}$) couple with each other leading to the splitting of the O−D stretch band into ω_1 and ω_2 (top). Isotopic dilution results in HOD species where the stretch and bend overtone modes are uncoupled thus merging the two bands into a single peak.

which the droplets are dispersed. The IR absorption modifies the recorded SF spectra in a nontrivial way. Nevertheless, recently, these effects have been theoretically described[22] and implemented to retrieve the true surface response in an SFS experiment.[23] The second challenge arises from the role of vibrational coupling in the spectral shape of water spectra. The frequency distributions and relative intensities measured in the SF spectra are influenced by both intermolecular and intramolecular coupling between water molecules. Thus, to extract the interfacial H-bonding structure, the vibrational coupling effects need to be minimized. While such experiments have been performed at the air/water interface,[24−31] implementing them in an SF scattering experiment is technologically different. As the nature of the interface (nanoscale, hydrophobic) is different from a planar extended air−water interface or bulk water, the results are expected to be different.

Here, we implement isotope dilution vibrational sum frequency scattering for the entire O−D stretch region of the vibrational spectrum of water. We characterize the structure of the hydrogen-bonding network next to 200 nm hexadecane droplets dispersed in pure water. The peak frequencies and intensity ratios reveal that water forms an overall stronger hydrogen-bonding network next to hydrophobic droplets compared to bulk and the air/water interface, which is apparent from three different metrics: The spectral shape of the nonisotopically diluted water compared to the spectral shape of the air−water interface as a function of temperature, the central peak position of the isotopically diluted OD spectrum (15% D_2O in H_2O), and the spectral shape of that spectrum, most notably the presence of a low-frequency mode. Half of the spectral width of the vibrational SFS spectrum is determined by the intra-/intermolecular coupling of water molecules, which is similar to bulk water. Examining the high-frequency part of the spectrum as a function of mole fraction of D_2O in H_2O, we determine that on top of the vibrationally coupled modes, there is a broad population (ca. 2640−2745 cm^{-1}) of uncoupled non-water-hydrogen-bonded modes.

RESULTS AND DISCUSSION

Nanodroplets of hexadecane with an average diameter of 200 nm (section S1, Figure S1) were prepared in different D_2O/H_2O mixtures using ultrasonication as described in the Materials and Methods (section S1). The D_2O/H_2O mixtures consisted of 15, 50, and 100 vol % D_2O in H_2O, leading to mixtures with 25% HOD, 2% D_2O, 73% H_2O; 50% HOD, 25% D_2O, 25% H_2O; and 100% D_2O, respectively. The vibrational SFS spectra of droplets were measured in the O−D stretch region using the SSP (S−SF, S-visible, P-IR) polarization combination. Since the IR beam is absorbed by D_2O as it travels through the sample cell (Figure 1A), each droplet will experience a different spectral excitation, eventually resulting in strongly modified SFS spectra.[22] Therefore, we first quantified the effects of linear absorption of the IR beam to retrieve the

https://doi.org/10.1021/acs.jpcb.2c01987
J. Phys. Chem. B 2022, 126, 3186−3192

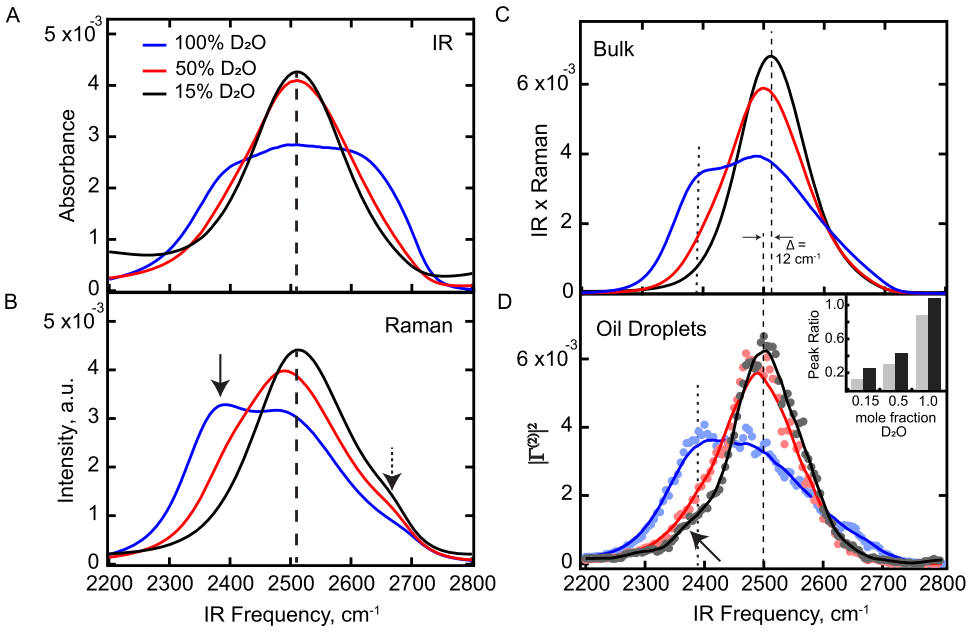

Figure 2. Isotopic dilution and the vibrational spectra of bulk and nanodroplet interfacial D_2O. (A) IR and (B) vertically polarized Raman spectra of different D_2O/H_2O mixtures containing 100 vol % D_2O (blue), 50 vol % D_2O (red), and 15 vol % D_2O (black). (C) Product of the vertically polarized Raman spectrum with the IR spectrum for different isotopic dilution ratios. (D) $|\Gamma^{(2)}|^2$ spectrum of oil droplets dispersed in D_2O/H_2O mixtures recorded using the SSP polarization combination. The solid lines represent the running average and are a guide to the eye. The vertical dashed line represents the peak frequency of the uncoupled O−D mode as seen in the spectrum of 15% D_2O. The vertical dotted lines indicate the presence of a strongly H-bonded O−D population at the oil droplet surface compared to bulk. The legends correspond to volume % of D_2O added in the mixture. The inset shows the 2395/2500 cm^{-1} peak ratio from the oil droplets (black) and bulk water (gray) at different D_2O/H_2O ratios. Note that all spectra are normalized to their area.

true interfacial response for oil droplets dispersed in water. The procedure used to convert the measured SF intensity to the true interfacial response, $|\Gamma^{(2)}|^2$, is described in Section S2 of the SI. $\Gamma^{(2)}$ is the effective second-order particle susceptibility that describes the spectral interfacial response of droplets dispersed in solution. $\Gamma^{(2)}$ is a function of the scattering angle (θ, defined as the angle between the scattered SF wavevector and that of the phase-matched direction, Figure 1A), the average radius (R) of the droplets, and the second-order surface susceptibility ($\chi^{(2)}$).[32−34]

SFS Spectrum of Water Next to an Oil Droplet. Figure 1B (blue spectrum) shows the obtained sum frequency $|\Gamma^{(2)}|^2$ spectrum of 2 vol% hexadecane droplets in D_2O.[23] The intensity between 2200 and 2800 cm^{-1} originates from the O−D stretch modes of interfacial D_2O molecules at the oil droplet surface. These interfacial vibrational modes include O−D stretches from water molecules with an asymmetric molecular orientation with respect to the surface normal. This anisotropy originates either from the interaction with the weak interfacial electrostatic field that arises from the charge on oil droplets, or from other nonelectrostatic interactions.[36] The broad shape of this spectrum is determined by a combination of effects: H-bonding, intermolecular, and intramolecular vibrational couplings. In the following, we decouple these effects to reveal the characteristics of the H-bonding network around oil droplets.

In water, an O−D oscillator can be situated in a strongly, weakly, or non-H-bonded environment and therefore can have different frequencies. The O−D stretch spectrum at the oil droplet surface has two broad features around ∼2395 and ∼2500 cm^{-1} (indicated by the dotted lines in Figure 1B). Reflection SFG measurements of the air−water interface[10] shows that the peak ratio between 2395 and 2500 cm^{-1} changes with temperature. These data are reproduced in the inset of Figure 1B and demonstrate that the 2395/2500 cm^{-1} ratio increases with decreasing temperature, and therefore reducing the temperature results in stronger H-bonding. Comparing these data from the air/water interface to the water spectrum at the oil nanodroplet interface, we observe a ratio (indicated by the blue square in the inset of Figure 1B) that corresponds to an equivalent air−water interface at 277 K. Therefore, at identical (room) temperatures, a stronger H-bonding network is observed at the oil droplet surface compared to the air/water interface.

Another difference between water at the oil nanodroplet and planar extended air/water interface is evident in the high-frequency region of the spectra. The characteristic sharp peak around 2745 cm^{-1} in the air/water interfacial spectrum originates from non-H-bonded/free O−D modes.[28,37] At the oil droplet surface, these non-H-bonded O−D modes are not clearly visible. Polarimetric SFS was recently used to study this spectrum in more detail.[23] Using spectra recorded with different polarization combinations in combination with group theory and nonlinear light scattering theory, it was possible to determine that there was a broad spectral distribution arising from water molecules that were not H-bonded to other water molecules.[23] This region overlaps with the asymmetric shoulder that starts at ∼2520 cm^{-1} and reaches ∼2800 cm^{-1}. It is indicated by the dotted-blue-filled Gaussian. In addition to a difference in H-bonding, the spectrum in Figure 1B is likely also influenced by intra- and intermolecular coupling. The vibrations of water molecules are not isolated and distributed among several water molecules and vibrational modes. Auer and Skinner[38] estimated in a computational study that each O−D vibrational mode is linked to up to 12

https://doi.org/10.1021/acs.jpcb.2c01987
J. Phys. Chem. B 2022, 126, 3186−3192

neighboring O−D oscillators that have similar vibrational energies. This interaction, known as intermolecular coupling, leads to a broadening of the O−D stretch spectrum (illustrated in Figure 1C).[38−40] Furthermore, the vibrational energy of water molecules can also be delocalized over different vibrational modes of the same molecule via intramolecular coupling: The O−D stretch modes and the overtone of D−O−D bending modes have similar vibrational energies and they are coupled with each other via Fermi resonance (Figure 1D). Intramolecular coupling leads to energy-level splitting and peak broadening of the O−D stretch vibrations (illustrated in Figure 1D).[24] To decouple the local H-bonding and vibrational coupling effects, we next describe isotopic dilution experiments for bulk (using IR, and Raman spectroscopy) and droplet interfacial water (using SFS). To disentangle structure from coupling, we use a volume ratio of D_2O of just 15% and probe the O−D oscillators. In this way, the vibrational coupling is minimized since the energy levels of the probed vibrational modes are now different from those that surround them (the O−H groups). Note that this does not disturb the configuration of the hydrogen-bond network itself.[38]

Bulk IR and Raman Isotopic Dilution Spectroscopy. We recorded IR and Raman spectra for D_2O/H_2O mixtures consisting of 15, 50, and 100 vol % D_2O in H_2O. They are shown in Figure 2A (IR) and 2B (Raman), respectively. Reducing the amount of O−D oscillators in the sample to a fraction of 0.15 reduces the intensity significantly. Facilitating the comparison of spectral shapes, all spectra in Figure 2 are normalized to their spectral area.

These bulk IR and Raman data are in agreement with published literature[38,41−43] and confirm that the IR spectrum of isolated HOD (15% D_2O in H_2O, black trace, Figure 2A) is centered around ∼2510 cm^{-1} (dashed line, Figure 2A), with a full width at half-maximum (FWHM) of ∼190 cm^{-1}, and thus narrower than the bulk water spectrum of 100% D_2O (blue trace, Figure 2A, ∼350 cm^{-1}). The wide distribution of vibrational frequencies in the IR spectrum of pure D_2O has contributions from H-bonding, intermolecular, and intramolecular coupling. In pure D_2O, the O−D vibrational mode of each water molecule is delocalized onto several neighboring water molecules (Figure 1C), resulting in the broadening and shift to lower frequencies. With isotopic dilution, the O−D oscillators are increasingly surrounded by H_2O molecules, thereby decreasing the intermolecular O−D coupling and thus the width of the O−D spectrum (Figure 1C, bottom; Figure 2A, red and black spectra). Moreover, the intramolecular coupling (Figure 1D) is also switched off since the frequency of the HOD bending overtone is ∼2900 cm^{-1} and is therefore no longer in resonance with the O−D stretch modes.[44] By minimizing intramolecular and intermolecular coupling effects, the IR spectrum of 15% D_2O (Figure 2A, black) reveals the different H-bonding environments present in bulk water: A change in width from 350 to 190 cm^{-1}, meaning that the width of the uncoupled spectrum is 0.54 times that of the coupled one.

The Raman spectrum of bulk water shows similar features with isotopic dilution (Figure 2B). Here, the spectral width decreases from ∼300 cm^{-1} for 100% D_2O to ∼195 cm^{-1} for 15% D_2O, showing that ∼1/3 of the spectral width arises from inter- and intramolecular coupling. The spectral shape of the vertically polarized Raman spectrum of 100% D_2O is clearly different from the IR spectrum (blue spectra in Figure 2A,B). IR and Raman spectral shapes are different because the angular factors in transition dipole and polarizability, respectively, determine the weights of different frequency components in the IR and Raman spectra.[38] The red side of the Raman spectrum at ∼2395 cm^{-1} has a distinct shoulder (solid arrow, Figure 2B), whereas such a feature is not present in the IR spectrum. Auer and Skinner calculated the IR and Raman line shapes of H_2O and suggested that this low-frequency shoulder is a collective vibrational mode resulting from the delocalization of O−H modes over several oscillators (up to 12 O−H oscillators in their computations).[38] The shoulder around 2650 cm^{-1} (Figure 2B, dotted arrow) that is more visible in the vertically polarized Raman spectra and less so in the IR spectra has previously been attributed to water molecules with non-H-bonded O−D modes.[38,45]

Since sum frequency generation involves a simultaneous IR and Raman transition[46,47] (Figure 1A), we computed the product of the IR and Raman spectra at different isotopic dilutions. Differences between the IR x Raman spectrum and the droplet $|\Gamma^{(2)}|^2$ spectra reveal information about the different interfacial molecular environments at the oil droplet/water interface compared to bulk water. Figure 2C shows the product of IR and vertically polarized Raman spectra in the absence of droplets at different isotopic dilution ratios. Similar to IR and Raman spectra, the product also shows increased spectral width for pure D_2O (FWHM ∼250 cm^{-1}) and spectral narrowing and blueshift with isotopic dilution (FWHM ∼130 cm^{-1}). The center peak frequency of the bulk uncoupled O−D stretch mode at 15% D_2O is 2512 cm^{-1}, and it has a full width at half-maximum (FWHM) of ∼130 cm^{-1}. Published reflection SF spectra of the isotopically diluted air/water interface[24,26] are very similar compared to the IR × Raman spectra of bulk water in Figure 2C, with a center frequency/FWHM combination of 2510/150 cm^{-1}. The H-bond network adjacent to the air−water interface was thus concluded to be very similar to that of bulk water.[26] For 100% D_2O, the IR × Raman shows two distinct features in the H-bonded OD region, similar to the SFG spectrum of the air/water interface. Schaefer et al. decomposed the effect of intra- and intermolecular coupling at the air/water interface and concluded that intramolecular coupling (Figure 1D) is responsible for the splitting of the OD stretch band into two (leading to the "modes" at 2395 and 2500 cm^{-1}), whereas intermolecular coupling (Figure 1C) was concluded to be primarily responsible for the spectral broadening.[29] However, the temperature dependence of Figure 1B shows that despite this coupling effect, there is also a different distribution of H-bonds around those frequencies. Thus, for bulk water and for the air−water interface, H-bond strength as well as inter- and intramolecular coupling contribute to the vibrational spectrum of water.

SFS Isotopic Dilution Spectroscopy of the Droplet Interface. Figure 2D shows the droplet $|\Gamma^{(2)}|^2$ spectra at different isotopic dilution ratios. Comparison between the blue spectra in Figure 2C,D reveals the inversion of the 2395/2500 cm^{-1} ratio on going from bulk water to interfacial water: At 100% D_2O, the 2500 cm^{-1} feature has a higher relative intensity compared to the 2395 cm^{-1} feature for bulk water, whereas the 2395 cm^{-1} feature is relatively more intense at the oil droplet surface (see also the inset of Figure 1B). The 2395/2500 cm^{-1} ratio for pure D_2O however can be due to a stronger H-bonding, vibrational coupling, or a combination of both. Inspection of the 15% D_2O spectra in Figure 2C,D reveals that a (smaller) shoulder around 2395 cm^{-1} remains at

https://doi.org/10.1021/acs.jpcb.2c01987
J. Phys. Chem. B 2022, 126, 3186−3192

the oil droplet surface even for the uncoupled O−D indicating the presence of a strongly H-bonded water population. In contrast, for bulk water, this asymmetric shoulder is completely absent. The inset of Figure 2D shows the 2395/2500 cm^{-1} peak intensity ratio for different D_2O/H_2O ratios. At all isotopic dilution ratios, the peak ratio is higher for the oil droplet surface compared to bulk water, indicating that the oil droplet interface induces more strongly H-bonded water molecules at the hydrophobic oil droplet surface, in agreement with the temperature dependence experiment (Figure 1B). Thus, on the oil nanodroplet interface, the doublet structure at 2395/2500 cm^{-1} is not purely due to vibrational coupling, and a fraction of more strongly hydrogen-bonded water molecules exists (in contrast to what has been concluded about the air−water interface[26]). This more strongly hydrogen-bonded environment is also apparent by comparing central frequencies of the isotope diluted spectra. The center frequency of the uncoupled O−D vibration at the nanodroplet interface is at 2500 cm^{-1}, whereas the uncoupled bulk O−D spectrum is centered at ∼2512 cm^{-1}. Compared to bulk water (and the air/water interface), there is thus a 10−12 cm^{-1} vibrational mode shift to lower frequencies.

Non-Water-H-Bonded O−D Modes. Comparing the SFS spectrum of the water adjacent to oil droplets to the reported spectrum of the air/water interface,[10,35,37] the biggest difference in Figure 1B occurs >2500 cm^{-1}. On a planar air/water interface, this high-frequency O−D population originates from non-H-bonded water molecules. On the oil droplet, if such a population is present, it could be red-shifted and merged with the broad H-bonded O−D continuum,[5] as investigated recently by polarimetric SFS.[23] Inspecting the SFS spectra from the droplets (Figure 2D), we note that there is still SFS intensity up to ∼2745 cm^{-1} for all three spectra. We investigate the nature of this water by analyzing the isotopic dilution spectra in more detail. Figure 3A shows the integrated spectral SF intensity for the different isotopic dilutions. If one assumes

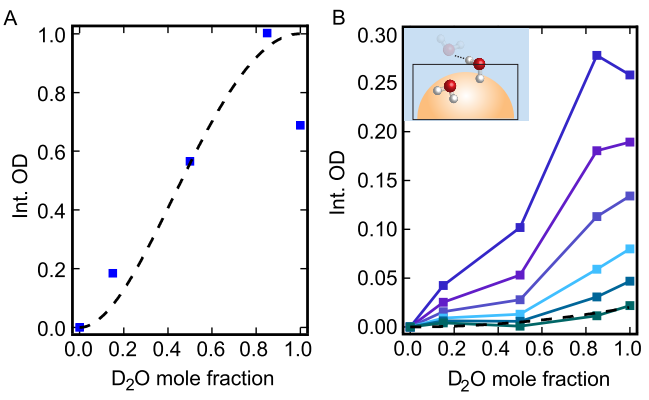

Figure 3. Identifying the non-H-bonded O−D population. (A) Integrated SF spectral intensity as a function of D_2O mole fraction in the mixture (blue squares). The square of the total amount of O−D oscillators is also plotted as an indication of the expected amount of intensity if all O−D oscillators were independent (dashed line). (B) Integrated SF spectra in different spectral regions (from top to bottom in the order): 2600−2800, 2620−2800, 2640−2800, 2660−2800, 2680−2800, and 2700−2800 cm^{-1}. The dashed line represents the square of the amount of interfacial D_2O, which would be responsible for uncoupled non-H-bonded O−D oscillator intensity. The inset shows an illustration of a non-water-H-bonded O−D mode that contributes to the high-frequency region of the SFS spectrum.

that every O−D group contributes in an identical manner to the SF spectrum, the integrated SF intensity can be approximated as the square of the total number of O−D oscillators. This curve is shown as the dashed line in Figure 3A. Comparing the SFS data to this curve, we observe that the maximum overall intensity is reached for the mixture of 85 vol % D_2O in H_2O and not for 100% D_2O. This means that in pure D_2O, vibrational coupling reduces the integral intensity of the SFS spectrum. In the high-frequency region of the spectrum, where one observes non-H-bonded water molecules, we expect to obtain a bigger contribution from D_2O compared to HOD since the vibrational frequency of non-H-bonded D_2O is higher than that of HOD.[28] To determine if non-H-bonded D_2O is indeed present, we integrate the SF spectra in different spectral regions of 2600−2800, 2620−2800, 2640−2800, 2660−2800, 2680−2800, and 2700−2800 cm^{-1}. Figure 3B shows the resultant integrated intensities plotted as a function of mole fraction of D_2O. As is the case in Figure 3A, the intensity in the high-frequency spectral region is smaller for lower mole fractions of D_2O. If uncoupled O−D of D_2O is present, the SFS intensity should increase monotonously with an increase in the amount of D_2O.[28] The dashed line in Figure 3A represents the square of the relative amount of D_2O in the sample, which represents the expected SF intensity. The spectral range 2600−2800 cm^{-1} maximizes at a D_2O volume fraction of 0.85, indicating that multiple species contribute to this part of the SFS spectrum (HOD as well as D_2O molecules). The spectral range >2640 cm^{-1} increases monotonously, indicating a smaller contribution of HOD molecules, while the range >2700 cm^{-1} follows the trend expected when only D_2O contributes to the SF response. This analysis reveals that the high-frequency part of the SFS spectrum of water adjacent to oil droplets contains non-water-H-bonded water molecules, even though they are not directly visible as a separate peak as in the air/water reflection SF spectrum. It should be noted that we are able to identify the isotopically pure D_2O component of the non-H-bonded O−D population due to the monotonous increase in intensity. This high-frequency spectral region has fewer overlapping resonances compared to the H-bonded part of the O−D stretch spectrum. However, intensity in the SFS spectra toward lower frequencies can further be complicated by overlapping resonances, presumably giving rise to the nonmonotonous trend that maximizes around D_2O volume fraction of 0.85.

Given that the monotonous increase in Figure 3B already starts at 2640 cm^{-1}, we conclude that there is a broad spectral region that contains D_2O molecules that are not H-bonded to other water molecules. Non-H-bonded water at the oil droplet interface can refer to multiple species: Truly free isolated water molecules, water molecules with a single free O−D group, and water molecules that interact with oil and not with water (Figure 3B inset). The first two are known to exist at the air/water interface and occupy a rather narrow spectral region around 2745 cm^{-1}. Water molecules that interact with oil are therefore the ones that most likely attribute to the broad spectral band down to ∼2600 cm^{-1} that can be discerned using isotopic dilution. This broad band agrees with the polarimetric SFS results.[23] In the latter study, concomitant SFS measurements of the C−H modes of the oil were also performed as were interfacial charge measurements. The combined data set revealed that charge transfer occurs from water to oil. Charge transfer not only produces a broad band of non-water H-bonded OD modes but also renders the oil droplet surface

https://doi.org/10.1021/acs.jpcb.2c01987
J. Phys. Chem. B 2022, 126, 3186−3192

negatively charged and thus stable. Additional simulations provided evidence for improper H-bonds between water and oil.[23] The measurements shown here confirm the presence of a broad distribution of non-water-H-bonded water molecules via a different, unrelated, set of experiments. Our data show that water is not only more strongly H-bonded to water at the oil−water interface but also participates in more diverse structures and interactions.

CONCLUSIONS

In summary, we provided an interfacial isotope dilution study on the O−D stretch mode of D_2O in contact with hydrophobic oil nanodroplets. We disentangled hydrogen-bonding and vibrational coupling effects of water next to hydrophobic oil droplets dispersed in water using isotopic dilution vibrational SFS spectroscopy. Correcting for IR absorption effects allows one to retrieve the $|\Gamma^{(2)}|^2$ spectrum from the measured SFS response. Analysis of the O−D stretch vibrational spectra as a function of temperature and isotopic dilution revealed the presence of more strongly hydrogen-bonded water molecules at the oil nanodroplet surface compared to the extended planar air/water interface as well as bulk water, through three different observations: A higher ratio of the 2395/2500 cm^{-1} modes at room temperature compared to temperature-dependent data taken at the air−water interface, a redshift in the vibrationally uncoupled SFS O−D mode spectrum, and a shoulder around 2395 cm^{-1} in the same uncoupled spectrum. The intra- and intermolecular vibrational coupling at the oil droplet surface was responsible for roughly half the spectral width of the SFS spectrum. This is similar to that of bulk water. The similarity between the structure of water next to a hydrophobic oil droplet, the planar extended air/water interface, and bulk water is not surprising: The O−H and O−D stretch modes are localized vibrations and the structure of water is for a large part determined by surrounding water (even at an interface). Therefore, the observed spectral differences are relatively small. This may change if one probes over a longer length scale. However, the difference reported here between the water in contact with a hydrophobic nanodroplet and bulk water is noticeably larger than the difference between bulk water and the air−water interface. As a token of this similarity and subtle difference, we found that non-water-H-bonded O−D species are present at the oil droplet surface via isotopic dilution experiments. Although not immediately evident from the nonisotopically diluted spectrum, from ∼2640 cm^{-1} and onward to higher frequencies, there are water molecules that are not hydrogen-bonded to other water molecules. The frequency distribution is broad compared to the planar air/water interface due to the charge transfer interactions with oil molecules, which were previously identified via a different set of experiments.[23]

ASSOCIATED CONTENT

Supporting Information

The Supporting Information is available free of charge at https://pubs.acs.org/doi/10.1021/acs.jpcb.2c01987.

Materials and Methods (S1) including chemicals, preparation of droplets, vibrational SFS, and the method of retrieving $|\Gamma^{(2)}|^2$ spectrum from measured SF intensity (S2) (PDF)

AUTHOR INFORMATION

Corresponding Author

S. Roke − *Laboratory for fundamental BioPhotonics, Institute of Bioengineering (IBI), School of Engineering (STI), Institute of Materials Science and Engineering (IMX), School of Engineering (STI), and Lausanne Centre for Ultrafast Science, École Polytechnique Fédérale de Lausanne (EPFL), CH-1015 Lausanne, Switzerland;* orcid.org/0000-0002-6062-7871; Email: sylvie.roke@epfl.ch

Authors

S. Pullanchery − *Laboratory for fundamental BioPhotonics, Institute of Bioengineering (IBI), School of Engineering (STI), École Polytechnique Fédérale de Lausanne (EPFL), CH-1015 Lausanne, Switzerland;* orcid.org/0000-0002-7011-0788

S. Kulik − *Laboratory for fundamental BioPhotonics, Institute of Bioengineering (IBI), School of Engineering (STI), École Polytechnique Fédérale de Lausanne (EPFL), CH-1015 Lausanne, Switzerland*

Complete contact information is available at: https://pubs.acs.org/10.1021/acs.jpcb.2c01987

Notes

The authors declare no competing financial interest.

ACKNOWLEDGMENTS

The authors thank the Julia Jacobi Foundation and the Swiss National Science Foundation (grant numbers 200021-182606-1). They also thank Prof. Dor Ben-Amotz for providing the Raman spectra.

REFERENCES

(1) Chandler, D. Interfaces and the driving force of hydrophobic assembly. *Nature* **2005**, *437*, 640−647.

(2) Tanford, C. The hydrophobic effect and the organization of living matter. *Science* **1978**, *200*, 1012.

(3) Lee, S. H.; Rossky, P. J. A comparison of the structure and dynamics of liquid water at hydrophobic and hydrophilic surfaces—a molecular dynamics simulation study. *J. Chem. Phys.* **1994**, *100*, 3334−3345.

(4) Iuchi, S.; Chen, H.; Paesani, F.; Voth, G. A. Hydrated excess proton at water−hydrophobic interfaces. *J. Phys. Chem. B* **2009**, *113*, 4017−4030.

(5) Ishiyama, T.; Sato, Y.; Morita, A. Interfacial structures and vibrational spectra at liquid/liquid boundaries: Molecular dynamics study of water/carbon tetrachloride and water/1,2-dichloroethane interfaces. *J. Phys. Chem. C* **2012**, *116*, 21439−21446.

(6) Poli, E.; Jong, K. H.; Hassanali, A. Charge transfer as a ubiquitous mechanism in determining the negative charge at hydrophobic interfaces. *Nat. Commun.* **2020**, *11*, No. 901.

(7) Brown, M. G.; Walker, D. S.; Raymond, E. A.; Richmond, G. L. Vibrational sum-frequency spectroscopy of alkane/water interfaces: Experiment and theoretical simulation. *J. Phys. Chem. B* **2003**, *107*, 237−244.

(8) Du, Q.; Freysz, E.; Shen, Y. R. Surface vibrational spectroscopic studies of hydrogen bonding and hydrophobicity. *Science* **1994**, *264*, 826.

(9) Scatena, L. F.; Brown, M. G.; Richmond, G. L. Water at hydrophobic surfaces: Weak hydrogen bonding and strong orientation effects. *Science* **2001**, *292*, 908.

(10) Strazdaite, S.; Versluis, J.; Backus, E. H. G.; Bakker, H. J. Enhanced ordering of water at hydrophobic surfaces. *J. Chem. Phys.* **2014**, *140*, No. 054711.

(11) Goebel, A.; Lunkenheimer, K. Interfacial tension of the water/n-alkane interface. *Langmuir* **1997**, *13*, 369−372.
(12) Del Cerro, C.; Jameson, G. J. The behavior of pentane, hexane, and heptane on water. *J. Colloid Interface Sci.* **1980**, *78*, 362−375.
(13) Beattie, J. K.; Djerdjev, A. M. The pristine oil/water interface: Surfactant-free hydroxide-charged emulsions. *Angew. Chem., Int. Ed.* **2004**, *43*, 3568−3571.
(14) Roke, S.; Roeterdink, W. G.; Wijnhoven, J. E. G. J.; Petukhov, A. V.; Kleyn, A. W.; Bonn, M. Vibrational sum frequency scattering from a submicron suspension. *Phys. Rev. Lett.* **2003**, *91*, No. 258302.
(15) de Aguiar, H. B.; de Beer, A. G. F.; Strader, M. L.; Roke, S. The interfacial tension of nanoscopic oil droplets in water is hardly affected by SDS surfactant. *J. Am. Chem. Soc.* **2010**, *132*, 2122−2123.
(16) Vácha, R.; Rick, S. W.; Jungwirth, P.; de Beer, A. G. F.; de Aguiar, H. B.; Samson, J.-S.; Roke, S. The orientation and charge of water at the hydrophobic oil droplet−water interface. *J. Am. Chem. Soc.* **2011**, *133*, 10204−10210.
(17) Samson, J.-S.; Scheu, R.; Smolentsev, N.; Rick, S. W.; Roke, S. Sum frequency spectroscopy of the hydrophobic nanodroplet/water interface: Absence of hydroxyl ion and dangling OH bond signatures. *Chem. Phys. Lett.* **2014**, *615*, 124−131.
(18) Carpenter, A. P.; Tran, E.; Altman, R. M.; Richmond, G. L. Formation and surface-stabilizing contributions to bare nano-emulsions created with negligible surface charge. *Proc. Natl. Acad. Sci. U.S.A.* **2019**, *116*, 9214.
(19) Jena, K. C.; Scheu, R.; Roke, S. Surface impurities are not responsible for the charge on the oil/water interface: A comment. *Angew. Chem., Int. Ed.* **2012**, *51*, 12938−12940.
(20) Okur, H. I.; Chen, Y.; Wilkins, D. M.; Roke, S. The Jones-Ray effect reinterpreted: Surface tension minima of low ionic strength electrolyte solutions are caused by electric field induced water-water correlations. *Chem. Phys. Lett.* **2017**, *684*, 433−442.
(21) Pullanchery, S.; Kulik, S.; Okur, H. I.; de Aguiar, H. B.; Roke, S. On the stability and necessary electrophoretic mobility of bare oil nanodroplets in water. *J. Chem. Phys.* **2020**, *152*, No. 241104.
(22) Kulik, S.; Pullanchery, S.; Roke, S. Vibrational sum frequency scattering in absorptive media: A theoretical case study of nano-objects in water. *J. Phys. Chem. C* **2020**, *124*, 23078−23085.
(23) Pullanchery, S.; Kulik, S.; Rehl, B.; Hassanali, A.; Roke, S. Charge transfer across C−H···O hydrogen bonds stabilizes oil droplets in water. *Science* **2021**, *374*, 1366−1370.
(24) Sovago, M.; Campen, R. K.; Wurpel, G. W. H.; Müller, M.; Bakker, H. J.; Bonn, M. Vibrational response of hydrogen-bonded interfacial water is dominated by intramolecular coupling. *Phys. Rev. Lett.* **2008**, *100*, No. 173901.
(25) Tian, C.-S.; Shen, Y. R. Isotopic dilution study of the water/vapor interface by phase-sensitive sum-frequency vibrational spectroscopy. *J. Am. Chem. Soc.* **2009**, *131*, 2790−2791.
(26) Sovago, M.; Kramer Campen, R.; Bakker, H. J.; Bonn, M. Hydrogen bonding strength of interfacial water determined with surface sum-frequency generation. *Chem. Phys. Lett.* **2009**, *470*, 7−12.
(27) Nihonyanagi, S.; Ishiyama, T.; Lee, T.-k.; Yamaguchi, S.; Bonn, M.; Morita, A.; Tahara, T. Unified molecular view of the air/water interface based on experimental and theoretical $\chi(2)$ spectra of an isotopically diluted water surface. *J. Am. Chem. Soc.* **2011**, *133*, 16875−16880.
(28) Stiopkin, I. V.; Weeraman, C.; Pieniazek, P. A.; Shalhout, F. Y.; Skinner, J. L.; Benderskii, A. V. Hydrogen bonding at the water surface revealed by isotopic dilution spectroscopy. *Nature* **2011**, *474*, 192−195.
(29) Schaefer, J.; Backus, E. H. G.; Nagata, Y.; Bonn, M. Both inter- and intramolecular coupling of O−H groups determine the vibrational response of the water/air interface. *J. Phys. Chem. Lett.* **2016**, *7*, 4591−4595.
(30) Xu, X.; Shen, Y. R.; Tian, C. Phase-sensitive sum frequency vibrational spectroscopic study of air/water interfaces: H2O, D2O, and diluted isotopic mixtures. *J. Chem. Phys.* **2019**, *150*, No. 144701.
(31) Ahmed, M.; Nojima, Y.; Nihonyanagi, S.; Yamaguchi, S.; Tahara, T. Comment on "Phase-sensitive sum frequency vibrational spectroscopic study of air/water interfaces: H2O, D2O, and diluted isotopic mixtures" [J. Chem. Phys. 150, 144701 (2019)]. *J. Chem. Phys.* **2020**, *152*, No. 237101.
(32) Roke, S.; Bonn, M.; Petukhov, A. V. Nonlinear optical scattering: The concept of effective susceptibility. *Phys. Rev. B* **2004**, *70*, No. 115106.
(33) de Beer, A. G. F.; Roke, S. Sum frequency generation scattering from the interface of an isotropic particle: Geometrical and chiral effects. *Phys. Rev. B* **2007**, *75*, No. 245438.
(34) Dadap, J. I.; de Aguiar, H. B.; Roke, S. Nonlinear light scattering from clusters and single particles. *J. Chem. Phys.* **2009**, *130*, No. 214710.
(35) Smolentsev, N.; Smit, W. J.; Bakker, H. J.; Roke, S. The interfacial structure of water droplets in a hydrophobic liquid. *Nat. Commun.* **2017**, *8*, No. 15548.
(36) de Beer, A. G. F.; Campen, R. K.; Roke, S. Separating surface structure and surface charge with second-harmonic and sum-frequency scattering. *Phys. Rev. B* **2010**, *82*, No. 235431.
(37) Du, Q.; Superfine, R.; Freysz, E.; Shen, Y. R. Vibrational spectroscopy of water at the vapor/water interface. *Phys. Rev. Lett.* **1993**, *70*, 2313−2316.
(38) Auer, B. M.; Skinner, J. L. IR and Raman spectra of liquid water: Theory and interpretation. *J. Chem. Phys.* **2008**, *128*, No. 224511.
(39) Ramasesha, K.; De Marco, L.; Mandal, A.; Tokmakoff, A. Water vibrations have strongly mixed intra- and intermolecular character. *Nat. Chem.* **2013**, *5*, 935−940.
(40) Woutersen, S.; Bakker, H. J. Resonant intermolecular transfer of vibrational energy in liquid water. *Nature* **1999**, *402*, 507−509.
(41) Corcelli, S. A.; Skinner, J. L. Infrared and Raman Line Shapes of Dilute HOD in Liquid H2O and D2O from 10 to 90 °C. *J. Phys. Chem. A* **2005**, *109*, 6154−6165.
(42) Maréchal, Y. Infrared spectra of water. I. Effect of temperature and of H/D isotopic dilution. *J. Chem. Phys.* **1991**, *95*, 5565−5573.
(43) Max, J.-J.; Chapados, C. Isotope effects in liquid water by infrared spectroscopy. *J. Chem. Phys.* **2002**, *116*, 4626−4642.
(44) Chuntonov, L.; Kumar, R.; Kuroda, D. G. Non-linear infrared spectroscopy of the water bending mode: direct experimental evidence of hydration shell reorganization? *Phys. Chem. Chem. Phys.* **2014**, *16*, 13172−13181.
(45) Lawrence, C. P.; Skinner, J. L. Vibrational spectroscopy of HOD in liquid D2O. III. Spectral diffusion, and hydrogen-bonding and rotational dynamics. *J. Chem. Phys.* **2003**, *118*, 264−272.
(46) Moad, A. J.; Simpson, G. J. A unified treatment of selection rules and symmetry relations for sum-frequency and second harmonic spectroscopies. *J. Phys. Chem. B* **2004**, *108*, 3548−3562.
(47) Hirose, C.; Akamatsu, N.; Domen, K. Formulas for the analysis of surface sum-frequency generation spectrum by CH stretching modes of methyl and methylene groups. *J. Chem. Phys.* **1992**, *96*, 997−1004.

https://doi.org/10.1021/acs.jpcb.2c01987
J. Phys. Chem. B 2022, 126, 3186−3192